ISSN 1063-7788, Physics of Atomic Nuclei, 2019, Vol. 82, No. 4, pp. 343–350. © Pleiades Publishing, Ltd., 2019.
Russian Text © The Author(s), 2019, published in Yadernaya Fizika, 2019, Vol. 82, No. 4, pp. 297–304.

NUCLEI
Experiment

Investigation of Inelastic Neutron Scattering on ^{27}Al Nuclei

N. A. Fedorov[1),2)*], T. Yu. Tretyakova[1),3)], V. M. Bystritsky[1)], Yu. N. Kopach[1)], I. N. Ruskov[1),4)], V. R. Skoy[1)], D. N. Grozdanov[1),4)], N. I. Zamyatin[1)], W. Dongming[1),5)], F. A. Aliev[1),6)], K. Hramco[1),7)], A. Kumar[8)], A. Gandhi[8)], S. Dabylova[1)], D. I. Yurkov[9)], and Yu. N. Barmakov[9)]

Received December 25, 2018; revised December 25, 2018; accepted December 25, 2018

Abstract—The results obtained by measuring the angular and energy distributions of gamma rays produced in reactions induced by the inelastic scattering of 14.1-MeV neutrons on ^{27}Al nuclei are presented. The respective measurements were performed by the tagged-neutron method in a beam from the ING-27 compact neutron generator. The angular distributions were obtained for gamma rays emitted from the 844-keV $1/2^+$, 1015-keV $3/2^+$, 2212-keV $7/2^+$, and 3004-keV $9/2^+$ states of ^{27}Al nuclei.

DOI: 10.1134/S1063778819040094

1. INTRODUCTION

The main objective of the TANGRA (TAgged Neutron and Gamma RAys) project, which is being implemented at the Laboratory of Neutron Physics at Joint Institute for Nuclear Research (JINR, Dubna) [1, 2], is to study in detail fast-neutron scattering on atomic nuclei by the tagged-neutron method. Measurement of $(n-\gamma)$ angular correlations in the inelastic scattering of 14.1 MeV neutrons furnishes additional information about the mechanism of interaction of the target nucleus with a projectile nucleon and about the effective nucleon–nucleon potential [3]. Information about processes of this type is substantially scantier than available data on inelastic charged-particle scattering on atomic nuclei. For theoretical studies in the realms of nuclear physics and nuclear astrophysics, a comparison of inelastic neutron scattering with the analogous reaction involving protons is of interest, since this makes it possible to explore isospin symmetry of nucleon–nucleon interactions. Isospin symmetry manifests itself most strongly in pairs of mirror nuclei, and this is the reason why the isotope ^{27}Al as a partner of the proton-rich nucleus of ^{27}Si in the isotopic doublet is a subject of vigorous investigations [4]. From the point of view of applications, the isotope ^{27}Al is of paramount importance since aluminum is widely used in practice. Interest in inelastic neutron scattering on ^{27}Al nuclei, as well as on nuclei of light and medium-mass elements, is motivated by an urgent need for refining experimental data obtained earlier. The underlying reason is that such reactions are applied in performing an express analysis of the elemental composition of rock [5, 6] and complex chemical compounds, in describing neutron-multiplication chains in nuclear power engineering, and in creating instruments for revealing hidden dangerous substances [7, 8].

The tagged-neutron method relies on detecting characteristic nuclear gamma radiation from inelastic neutron interaction with nuclei of the substance under study in coincidence with alpha particles originating from the binary reaction

$$d + t \to n(14.1\ \text{MeV}) + \alpha(3.5\ \text{MeV}), \qquad (1)$$

whose products move in opposite directions in the c.m. frame. Knowing the alpha-particle emission direction, one can therefore reconstruct the direction of motion of the outgoing neutron—that is, tag it. In practice, neutron tagging is accomplished by means

[1)]Joint Institute for Nuclear Research, Dubna, Moscow oblast, 141980 Russia.
[2)]Faculty of Physics, Moscow State University, Moscow, 119991 Russia.
[3)]Skobeltsyn Institute of Nuclear Physics, Moscow State University, Moscow, 119991 Russia.
[4)]Institute for Nuclear Research and Nuclear Energy, Bulgarian Academy of Sciences, BG-1784 Sofia, Bulgaria.
[5)]Xian Jiaotong University, 28 Xianning W Rd, Jiao Da Shang Ye Jie Qu, Beilin Qu, Xian Shi, Shaanxi Sheng, 718900 China.
[6)]Institute of Geology and Geophysics, Azerbaijan National Academy of Sciences, AZ1143 Baku, Azerbaijan.
[7)]Institute of Chemistry, Academy of Sciences of Moldova, MD-2028 Kishinev, Moldova.
[8)]Banaras Hindu University, Ajagara, Varanasi, Uttar Pradesh 221005, India.
[9)]Dukhov All-Russia Research Institute of Automatics (VNIIA), Moscow, 127055 Russia.
[*]E-mail: na.fedorov@physics.msu.ru

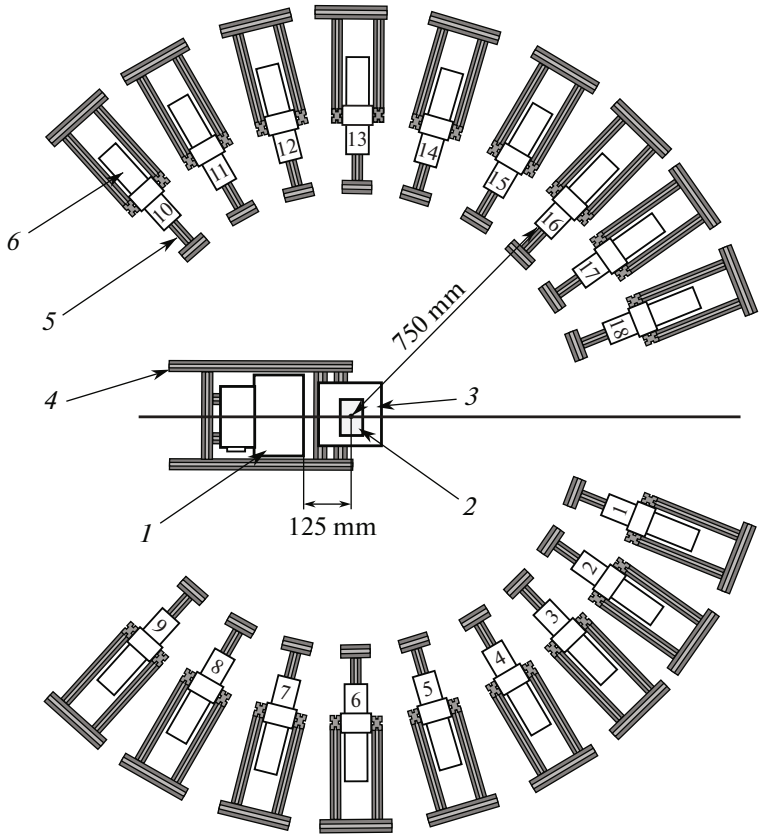

Fig. 1. Layout of the TANGRA experimental setup: (*1*) ING-27 neutron generator, (*2*) target, (*3*) target holder, (*4*) aluminum frame of the setup, (*5*) support for the gamma-ray detector, and (*6*) gamma-ray detector.

of a position-sensitive multipixel alpha-particle detector imbedded in the neutron generator. Alpha-particle detection also permits determining the intensity of the tagged-neutron flux and implementing the (α,γ) coincidence scheme, this reducing substantially the contribution of background events to the resulting gamma-ray spectra. Knowledge of the number of tagged neutrons incident to the target, the number of (n,γ) coincidences, the target dimensions, and the detection efficiency for gamma rays of characteristic nuclear radiation makes it possible to determine correctly the differential and total cross sections for processes in which inelastic neutron scattering on nuclei of the isotopes being studied leads to the excitation of specific nuclear levels. The possibility of monitoring the flux of tagged neutrons incident to the sample under study (in the present implementation of the experiment, there are 64 independent beams of tagged neutrons) and efficiently suppressing the contribution of background events to the resulting gamma-ray spectra is an important advantage of the tagged-neutron method.

2. IMPLEMENTATION OF THE EXPERIMENT

The TANGRA setup, whose layout is shown in Fig. 1, was created at JINR in order to study neutron–nucleus reactions. The ING-27 compact neutron generator operating in a continuous mode and ensuring the acceleration of deuterons to an energy of 80 to 100 keV and their focusing onto a tritium target is used as a source of tagged neutrons. The maximum intensity of the neutron flux in 4π geometry provided by the generator is 5×10^7 s^{-1}. Alpha particles of energy 3.5 MeV are recorded by a 64-pixel silicon detector embedded in the generator, characterized by pixel dimensions of 6×6 mm^2, and positioned at a distance 100 mm from the tritium target. Eighteen scintillation detectors based on BGO crystals 76 mm in diameter and 65 mm thick are used to record gamma rays. The gamma-ray detectors are arranged in a horizontal plane along a circle of radius 750 mm with an angular step of 14°. In contrast to the earlier setup version described in [9], the present configuration does not feature an additional passive collimation of the neutron beam incident to the sample exposed to neutrons, and this makes it possible to reduce the distance from the neutron-generator target to the center of the sample under study to 169 mm and to employ efficiently a larger number of tagged beams. Events corresponding to neutron–nucleus reactions in the

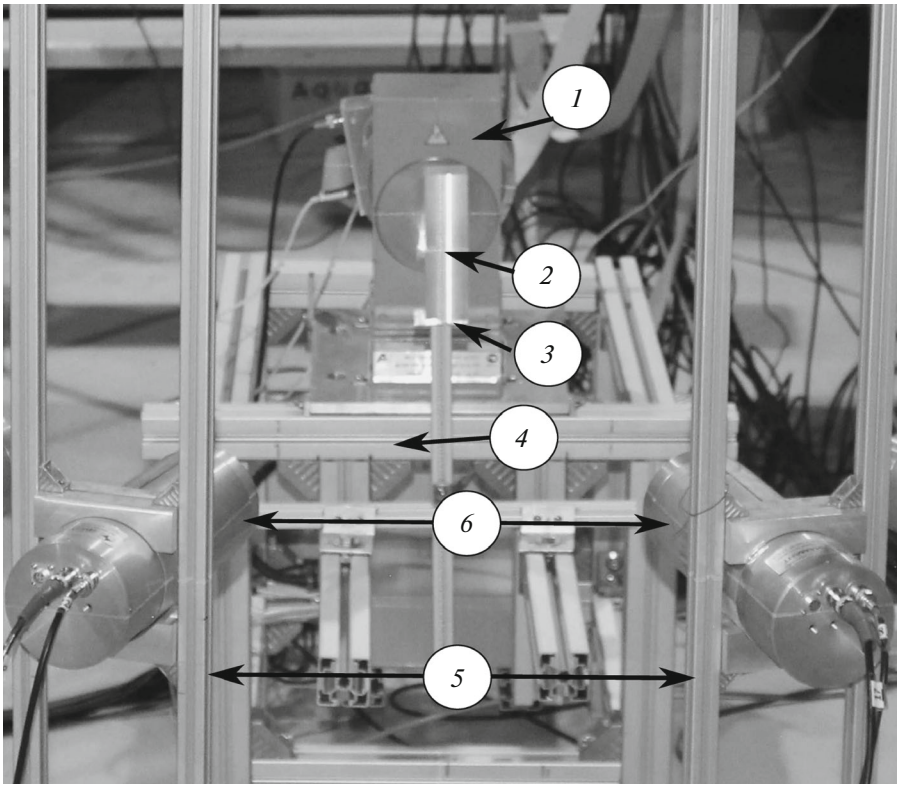

Fig. 2. Sample arranged in the experimental setup. The notation is identical to that in Fig. 1.

sample are selected on the basis of time-of-flight data: events lying in a rather narrow time interval whose beginning is specified by the instant of alpha-particle detection by the multipixel alpha-particle detector of the neutron generator are selected in order to construct the required energy spectra. This permits an efficient separation of gamma rays recorded by the gamma-ray detector and neutrons in the time of flight. A computer equipped with two analog-to-digital converters (ADCM-16) [10] is used for data acquisition and preliminary analysis.

In order to perform a correct measurement of angular distributions of gamma rays, it is necessary to estimate the effect of gamma-ray and neutron absorption and rescattering within the sample under study. For this purpose, a Monte Carlo simulation of our experiment with different-size samples was performed on the basis of the GEANT4 code package. For optimum target dimensions, we took those for which the change in the angular distribution of gamma rays (originating from reactions induced by inelastic neutron scattering on nuclei of the substances under study) because of variations in the geometric parameters of the sample did not exceed 10%.

The following procedure was used to determine the effect of sample dimensions on the resulting angular distribution: (i) Neutrons introduced according to the measured profiles of tagged beams [11] were used as initial particles. (ii) The interaction of neutrons and gamma ray with the substances of the target and gamma-ray detectors was described in terms of the (Physics List) "QGSP_BIC" parameters set [12], which is included by default in the GEANT4 package. (iii) The angular distribution of gamma rays produced in neutron interaction with sample matter and generated by GEANT4 was replaced in an ad hoc manner by an isotropic distribution. This simulation revealed that a sample $4 \times 4 \times 14$ cm^3 in size makes a rather small contribution to the anisotropy; therefore, we performed our experiment by employing a sample of precisely this size. A photograph of the setup in which the sample is installed is shown in Fig. 2.

3. DATA PROCESSING

Signals coming from alpha-particle and gamma-ray detectors of the setup were digitized by means of the ADCM block and were logged in the computer hard disk, whereupon they were analyzed via constructing time and amplitude spectra of events in which the detected neutrons and gamma rays are separated in time of flight.

The time distribution in Fig. 3 exhibits two peaks: peak *1* owes its existence to the detection of characteristic gamma radiation from ^{27}Al nuclei, while

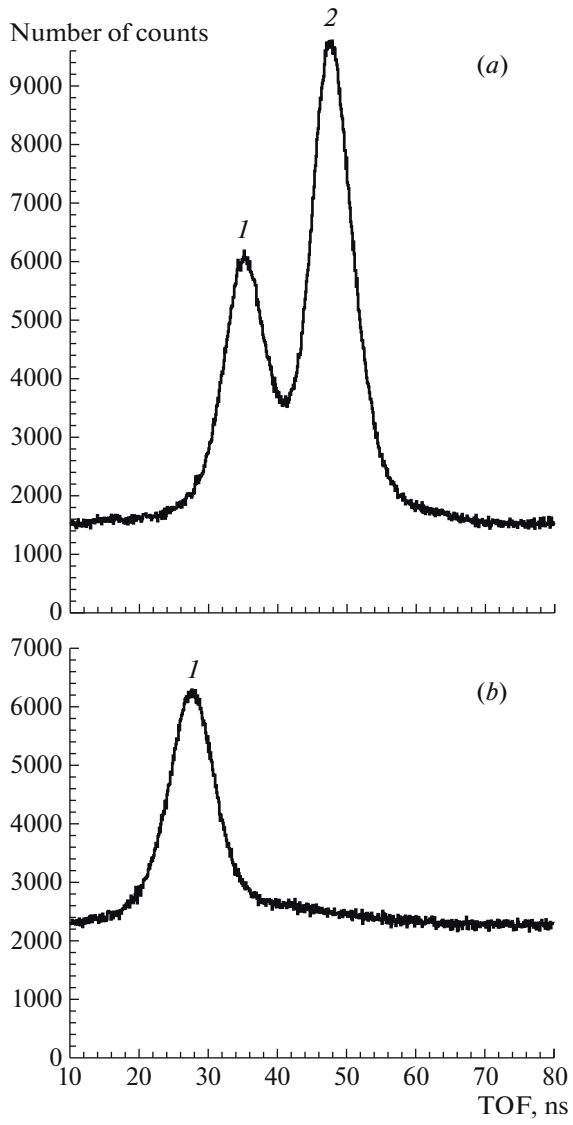

Fig. 3. Time spectra for detectors (*a*) no. 1 and (*b*) no. 6. In either spectrum, peak *1* corresponds to gamma rays. In Fig. 3*a*, peak *2* corresponds to neutrons.

peak *2* corresponds to the detection of neutrons that hit the detector. The counting rate for direct tagged neutrons is substantially higher in detector no. 1 than in detector no. 6, since the latter lies off the region of propagation of the tagged-neutron beams; therefore, there is no peak corresponding to neutrons in the time spectrum of events from detector no. 6.

Energy spectra are constructed for events falling within the time window corresponding to gamma-ray detection. In contrast to our preceding study reported in [13], where a 6×6 matrix of pixels of the alpha-particle detector was the source of start signals, we decided on employing signals from all pixels in the present experiment that belong to the four vertical strips (X strips) nearest to the axis of the system. This decision was motivated by the following two circumstances. First, the geometric dimensions of the sample are bounded: the observed anisotropy of gamma radiation should not be distorted substantially by gamma-ray and neutron interaction with sample matter. Second, the gamma-ray detectors lie in a horizontal plane, and the angle between the direction of emission of a detected gamma ray and the direction of the tagged neutron beam depends only slightly on the vertical coordinate of a pixel on a strip. The latter circumstance permitted grouping all pixels on vertical strips, with the result that it became possible to employ X-strip–gamma-detector combinations in subsequent data processing.

Information about the number of events corresponding to gamma-ray emission upon the transition of a target nucleus from a specific excited state to a state at a lower excitation energy is extracted from the energy spectra obtained in the way outlined above. Only those events that lie within the peak of total absorption of the gamma-ray energy by the detector matter or within the single-emission peak are usually taken into account.

The energy resolution of the BGO gamma-ray detectors (approximately 10.4% at $E_\gamma = 662$ keV) is insufficient for precisely identifying peaks in the energy spectra; therefore, we have performed a similar experiment with the aid of a high-purity germanium (HPGe) detector, which possesses a substantially higher energy resolution (approximately 3.4% at $E_\gamma = 662$ keV). A comparison of the energy spectra obtained with the BGO and HPGe detectors is illustrated in Fig. 4. Since the energy resolution of the BGO detectors leads to a substantial broadening of the peaks, only for the main, most intense, transitions is it possible to perform a reliable identification and, accordingly, to obtain results for the angular distribution of gamma rays. The gamma-ray energies for the respective peaks are indicated in Fig. 4.

In order to describe quantitatively the anisotropy of the angular distribution of gamma rays, it is common practice to introduce the anisotropy parameter $W(\theta)$. The experimental angular distributions of gamma rays are approximated by an expansion in terms of Legendre polynomials; that is,

$$W(\theta) = 1 + \sum_{i=2}^{2J} a_i P_i(\cos\theta), \qquad (2)$$

where a_i are expansion coefficients, J is the multipolarity of the respective gamma transition, and the summation index i takes only even values.

Information about the number of events corresponding to each gamma transition needs corrections because of gamma-ray absorption and rescattering

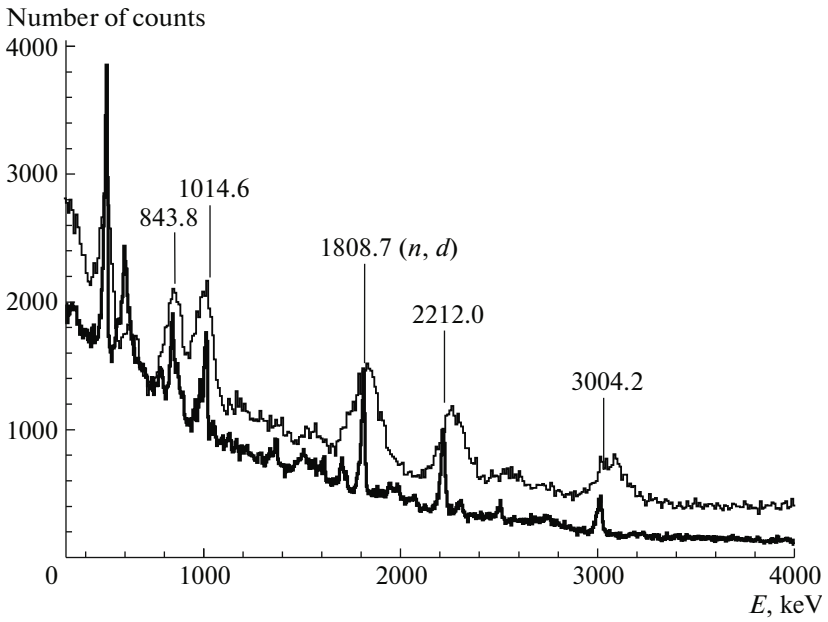

Fig. 4. Energy spectra measured by the (thin curve) BGO and (thick curve) HPGe detectors. The energy values (in keV units) are indicated for the most intense peaks in the spectra from the BGO detector.

in the sample. The ultimate angular anisotropy was determined according to the formula

$$W(\theta) = \frac{W_{\text{exp}}(\theta)}{K(\theta)}, \qquad (3)$$

where $K(\theta)$ stands for the dependence of the gamma-ray flux-reduction factor on the detector number for each strip. The reduction factor was evaluated by means of the GEANT4 code package according to the procedure outlined above. By way of example, Fig. 5 gives the gamma-ray flux-reduction factors for strip no. 3 and strip no. 4. One can see that gamma-ray and neutron interaction with sample matter may distort substantially the observed angular distribution in the case where a tagged beam does not intersect the sample center (in the case being considered, beam no. 3 goes through the center, while beam no. 4 does not).

4. RESULTS

In the experiment with HPGe detectors, we observed 18 gamma transitions corresponding to the (n, n'), (n, p), and (n, d) reactions on ^{27}Al nuclei. The energies of gamma rays and the reactions in which these gamma rays were emitted are listed in Table 1. Earlier, the most detailed spectrum of gamma radiation in the reaction $^{27}\text{Al}(n, x\gamma)$ induced by 14.9-MeV neutrons was obtained in [14]. Also, the differential cross sections were determined there for 26 discrete lines in the energy (E_γ) range between 90 and 3005 keV at three fixed values of the scattering angle; seven of these lines refer to the reaction $^{27}\text{Al}(n, n')^{27}\text{Al}$. In relation to the list presented in [14], all transitions associated with the (n, n') reaction and the majority of the gamma transitions from the (n, p) and (n, d) reactions were determined in our experiment. Additionally, the lines

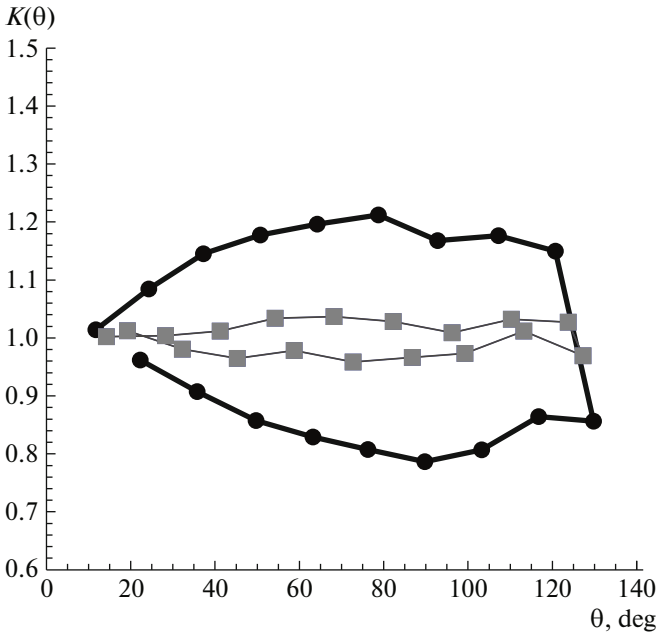

Fig. 5. Correction factors $K(\theta)$ for (thick curve, circles) strip no. 4 and (thin curve, boxes) strip no. 3. The points on display correspond to individual BGO detectors.

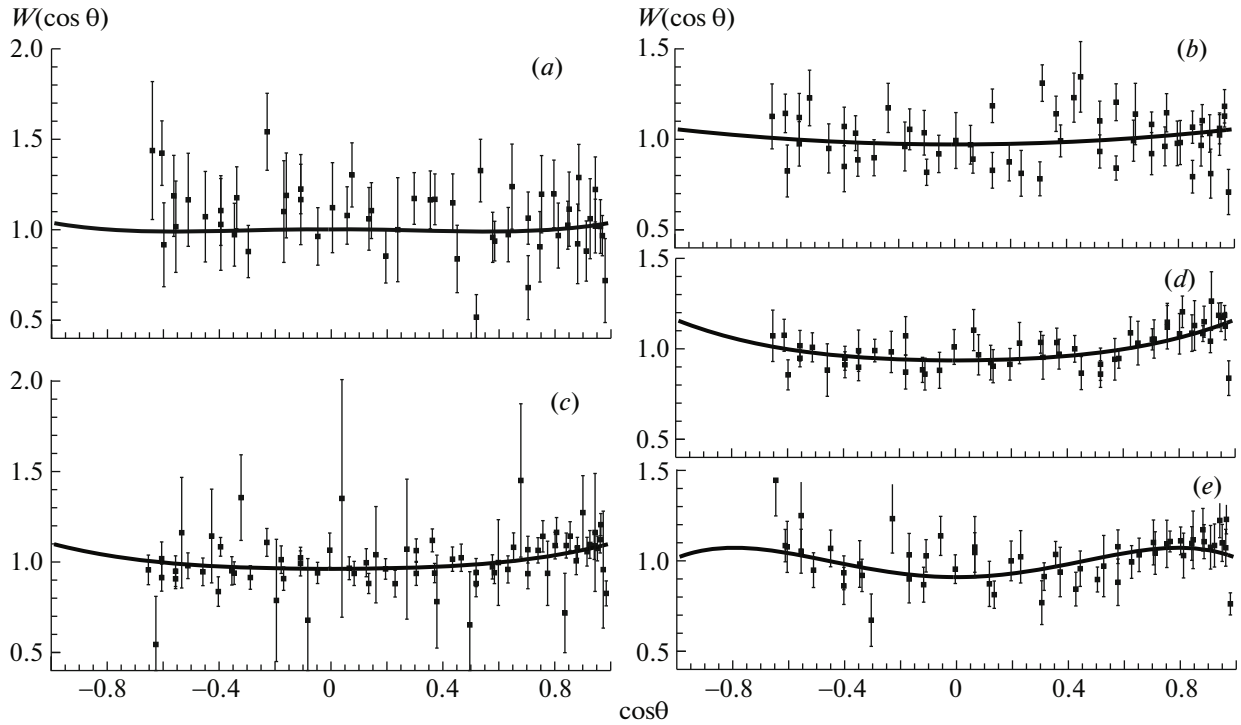

Fig. 6. Angular distribution of gamma rays emitted in processes where the scattering of 14.1-MeV neutrons on ^{27}Al nuclei leads to the excitation of the (a) level at 844 keV [(n, n') reaction], (b) level at 1015 keV [(n, n') reaction], and (c) level at 1809 keV [(n, d) reaction], as well as the levels at (d) 2212 keV and (e) 3004 keV [(n, n') reaction].

at $E_\gamma = 1506$, 3203, and 4580 keV corresponding to the $11/2^+(4510\,\text{keV}) \to 9/2^+(3004\,\text{keV})$, $1/2^-(4054\,\text{keV}) \to 1/2^+$ (844 keV), and $7/2^+(4580\,\text{keV}) \to 5/2^+(\text{g. s.})$ transitions in ^{27}Al were identified in our experiment.

We have obtained the angular distribution of gamma rays for the four most intense lines associated with the reaction $^{27}\text{Al}(n, n')$; their energies are $E_\gamma =$ 846, 1015, 2212, and 3004 keV. We have also obtained data on the angular distribution of gamma rays from the reaction $^{27}\text{Al}(n, d)^{26}\text{Mg}$ at $E_\gamma = 1809$ keV. Despite a large number of experiments performed earlier and devoted to measuring cross sections for gamma rays in the reaction $^{27}\text{Al}(n, n')^{27}\text{Al}$ at the neutron energy of 14 MeV [14–17], our attempts at finding information in databases about angular distributions of emitted gamma rays were futile. The angular distributions presented in [18] were obtained at the neutron energy of $E_n = 3.5$ MeV. A pronounced anisotropy was observed for 2212- and 3004-keV gamma rays and was found to be about 20%.

The gamma-ray angular distributions obtained in our experiment are similar. In Fig. 6, the experimental values determined for anisotropy parameter $W(\cos\theta)$ in (2) from an analysis of events lying within the total-absorption peak are given along with their analytic approximation in terms of Legendre polynomials. The coefficients a_i are compared in Table 2 with their model estimates obtained here within the approach relying on the compound-nucleus model according to the formulas presented in [19]. If the transition being considered proceeds from a state whose spin has a value smaller than the ground-state spin, then the angular distribution of gamma rays originating from this transition should have a rather small anisotropy. Accordingly, both the experimental results and the model estimates for the $E_\gamma = 846$ keV ($1/2^+$) and $E_\gamma = 1015$ keV ($3/2^+$) transitions correspond to an isotropic distribution. The experimentally observed isotropy of the distribution of 846-keV gamma rays is confirmed by model estimations; therefore, one can employ it as a criterion of correctness of experimental-data processing. The multipolarity of the $E_\gamma = 1015$ keV and $E_\gamma = 2212$ keV transitions is mixed, $M1 + E2$, which complicates the calculation of their anisotropy. In our present calculations, we assumed that the multipolarity of 1015-keV gamma rays was $M1$ and that the multipolarity of 2212-keV gamma rays was $E2$. The anisotropy of the 2212- and 3004-keV transitions is quite pronounced, 20%, the experimental results being in good agreement with model estimates.

Table 1. Gamma transitions observed experimentally [the gamma-ray energy E_γ (in keV units) and the respective activation reaction are indicated for each transition, along with energies and spin–parities of the initial, E_i (in keV units) and J_i^P, and final, E_f (in keV units) and J_f^P, states; boldface type is used for transitions in which angular distributions were determined]

E_γ	Reaction	E, J_i^P	E, J_f^P
472	^{27}Al$(n,\alpha)^{24}$Na	472(1^+)	0(4^+)
792	^{27}Al$(n,n')^{27}$Al	3004$(9/2^+)$	2211$(7/2^+)$
844	**^{27}Al$(n,n')^{27}$Al**	**844(**$1/2^+$**)**	**0(**$5/2^+$**)**
874	^{27}Al$(n,a)^{24}$Na	1346(1^+)	472(1^+)
985	^{27}Al$(n,p)^{27}$Mg	985$(3/2^+)$	0$(1/2^+)$
1014	**^{27}Al$(n,n')^{27}$Al**	**1014(**$3/2^+$**)**	**0(**$5/2^+$**)**
1506	^{27}Al$(n,n')^{27}$Al	4510$(11/2^+)$	3004$(9/2^+)$
1698	^{27}Al$(n,p)^{27}$Mg	1698$(5/2^+)$	0$(1/2^+)$
1720	^{27}Al$(n,n')^{27}$Al	2735$(5/2^+)$	1014$(3/2^+)$
1809	**^{27}Al$(n,d)^{26}$Mg**	**1809(**2^+**)**	**0(**0^+**)**
1940	^{27}Al$(n,p)^{27}$Mg	1940$(5/2^+)$	0$(1/2^+)$
2063	^{27}Al$(n,p)^{27}$Mg	3761$(5/2^-, 7/2^-)$	1699$(5/2^+)$
2211	**^{27}Al$(n,n')^{27}$Al**	**2211(**$7/2^+$**)**	**0(**$1/2^+$**)**
2298	^{27}Al$(n,n')^{27}$Al	4510$(11/2^+)$	2211$(7/2^+)$
2506	^{27}Al$(n,p)^{27}$Mg	3491$(3/2^+, 5/2^+)$	985$(3/2^+)$
3004	**^{27}Al$(n,n')^{27}$Al**	**3004(**$9/2^+$**)**	**0(**$1/2^+$**)**
3203	^{27}Al$(n,n')^{27}$Al	4054$(1/2^-)$	844$(1/2^+)$
4580	^{27}Al$(n,n')^{27}$Al	4580$(7/2^+)$	0$(5/2^+)$

Table 2. Coefficients in the expansion in terms of Legendre polynomials for the anisotropy of the angular distribution of gamma radiation in the approximation of experimental data (experiment) and in model calculations (calculation)

E_γ, keV	Experiment		Calculation	
	a_2	a_4	$a_{2\text{th}}$	$a_{4\text{th}}$
845	0.015 ± 0.2	0.05 ± 0.2	0	0
1015	0.06 ± 0.03		-0.015	
1805	0.09 ± 0.03	0.02 ± 0.03	–	–
2215	0.14 ± 0.02	0.02 ± 0.03	0.09	0
3005	0.11 ± 0.03	-0.09 ± 0.04	0.17	0.0013

5. CONCLUSIONS

The reactions induced by the inelastic scattering of 14.1-MeV neutrons on aluminum nuclei have been studied at the TANGRA experimental setup by employing tagged neutrons from the ING-27 compact neutron generator. The data subjected to the present analysis included those obtained with several tagged beams, and this made it possible to improve the statistical conditions of the experiment and to measure the anisotropy of gamma radiation with a good spatial resolution. Nevertheless, the data-processing procedure employed here still requires improvements—in particular, the use of the detector-response function would make it possible to determine peak areas in the energy spectra to a higher degree of precision.

REFERENCES

1. I. Ruskov, Yu. N. Kopatch, V. M. Bystritsky, V. Skoy, V. Shvetsov, F.-J. Hambsch, S. Oberstedt, R. Capote, P. V. Sedyshev, D. Grozdanov, I. Zh. Ivanov, V. Yu. Aleksakhin, E. P. Bogolubov, Yu. N. Barmakov, S. V. Khabarov, A. V. Krasnoperov, et al., Phys. Proc. **64**, 163 (2015).
2. V. M. Bystritsky, V. Valkovich, D. N. Grozdanov, A. O. Zontikov, I. Zh. Ivanov, Yu. N. Kopach, A. R. Krylov, Yu. N. Rogov, I. N. Ruskov, M. G. Sapozhnikov, V. R. Skoi, and V. N. Shvetsov, Phys. Part. Nucl. Lett. **12**, 325 (2015).
3. W. Hauser and H. Feshbach, Phys. Rev. **87**, 366 (1952).
4. G. Lotay, P. J. Woods, D. Seweryniak, M. P. Carpenter, H. M. David, R. V. F. Janssens, and S. Zhu, Phys. Rev. C **84**, 035802 (2011).
5. V. Yu. Alekhakhin, V. M. Bystritsky, N. I. Zamyatin, E. V. Zubarev, A. V. Krasnoperov, V. L. Rapatskiy, Yu. N. Rogov, A. B. Sadovsky, A. V. Salamatin, R. A. Salmin, M. G. Sapozhnikov, V. M. Slepnev, S. V. Khabarov, E. A. Razinkov, O. G. Tarasov, and G. M. Nikitin, Nucl. Instrum. Methods Phys. Res., Sect. A **785**, 9 (2015).
6. U. Waldschlaeger, Spectrochim. Acta, B **61**, 1115 (2006).
7. S. Pesente, G. Nebbia, M. Lunardon, G. Viesti, D. Sudac, K. Nad, S. Blagus, and V. Valkovic, Nucl. Instrum. Methods Phys. Res., Sect. A **531**, 657 (2004).
8. V. M. Bystritsky, V. V. Gerasimov, V. G. Kadyshevsky, A. P. Kobzev, A. A. Nozdrin, Yu. N. Rogov, V. L. Rapatsky, A. B. Sadovsky, A. V. Salamatin, M. G. Sapozhnikov, A. N. Sissakian, I. V. Slepnev, V. M. Slepnev, V. A. Utkin, N. A. Zamyatin, A. N. Peredery, et al., Phys. Part. Nucl. Lett. **5**, 441 (2008).
9. V. M. Bystritsky, D. N. Grozdanov, A. O. Zontikov, Yu. N. Kopach, Yu. N. Rogov, I. N. Ruskov, A. B. Sadovsky, V. R. Skoy, Yu. N. Barmakov, E. P. Bogolyubov, V. I. Ryzhkov, and D. I. Yurkov, Phys. Part. Nucl. Lett. **13**, 504 (2016).
10. ADCM-16 Description. http://afi.jinr.ru/ADCM16-LTC.
11. TANGRA Collab. (N. I. Zamyatin, V. M. Bystritsky, Y. N. Kopach, et al.), Nucl. Instrum. Methods Phys. Res., Sect. A **898**, 46 (2018).
12. Reference Physics Lists. https://geant4.web.cern.ch/node/155.

13. D. N. Grozdanov, N. A. Fedorov, V. M. Bystritski, Yu. N. Kopach, I. N. Ruskov, V. R. Skoy, T. Yu. Tretyakova, N. I. Zamyatin, D. Wang, F. A. Aliev, K. Hramco, A. Gandhi, A. Kumar, S. Dabylova, E. P. Bogolyubov, and Yu. N. Barmakov, Phys. At. Nucl. **81**, 588 (2018).
14. H. Zhou and G. Huang, Nucl. Sci. Eng. **125**, 61 (1997).
15. S. P. Simakov, A. Pavlik, H. Vonach, and S. Hlavac, INDC(CCP)-413 (IAEA NDS, Vienna, 1998).
16. S. Hlavac, L. Dostal, I. Turzo, A. Pavlik, and H. Vonach, Nucl. Sci. Eng. **125**, 196 (1997).
17. F. C. Engesser and W. E. Thompson, J. Nucl. Energy **21**, 487 (1967).
18. K. C. Chung, D. E. Velkley, J. D. Brandenberger, and M. T. McEllistrem, Nucl. Phys. A **115**, 476 (1968).
19. E. Sheldon and P. Gantenbein, Z. Phys. **18**, 397 (1967).